

# A simple method to estimate the $pK_a$ values of four fluorescent proteins based on measuring their pH-dependent absorbance spectra

Thi Yen Hang Bui\*, The Nga Tran

## ABSTRACT

**Introduction:** The Nobel Prize in Chemistry 2014 greatly recognized the application of fluorescent proteins (FPs) in superresolution imaging techniques. Subsequently, there has been a significant surge in FP-related investigations. Reversibly photoswitchable fluorescent proteins (rsFPs) are currently attracting much interest from scientists worldwide because of their unique ability to switch between bright and dark states. The pH-dependent photophysical behavior of rsFPs is mostly controlled by the equilibrium between four distinct states of the chromophores in FPs: *trans*-protonated, *trans*-deprotonated, *cis*-protonated, and *trans*-deprotonated. Thus, the  $pK_a$  values of rsFP in general and its chromophore, in particular, are crucial factors in determining the fluorescence output of the settings containing rsFPs in different environments. **Methods:** Here, we measured the absorbance spectra of four rsFPs in various buffers with different pH values to estimate their chromophore  $pK_a$ s. The relationship between the absorbance peak values for the anionic chromophore and pH is plotted, resulting in a sigmoid curve. Then, the apparent  $pK_a$  of the chromophore is obtained by determining the inflection point of this curve. **Results:** The  $pK_a$  values for the *cis*-chromophores of two rsFPs (GMarsQ and Skyran-S) were obtained. Specifically, the  $pK_a$  values for the *trans*-state of the chromophore in three rsFPs (Dronpa, GMarsQ, and rsEGFP2) were also estimated; these values have rarely been published. **Conclusions:** This approach is quite straightforward but effective, enabling us to quickly estimate the  $pK_a$  values of FPs generally and rsFPs specifically.

**Key words:** reversibly photoswitchable fluorescent proteins, dissociation constants

## INTRODUCTION

Green fluorescent protein (GFP) from *Aequorea victoria* was the first fluorescent protein discovered in 1962<sup>1</sup>. After successful cloning of the GFP gene in 1992, GFP-like proteins or fluorescent proteins (FPs) have been widely used as "smart labels" in many biology-related studies<sup>2-5</sup>. As FPs are genetically encoded fluorophores, they are highly specific for labeling and tracking cellular structures or proteins within living cells by using superresolution microscopy techniques<sup>6-8</sup>. In general, all FPs share a typical architecture motif with the shape of a  $\beta$ -can, which is constructed of 11  $\beta$ -strands surrounding an  $\alpha$ -helix (Figure 1A). The chromophore located at the center of the  $\alpha$ -helix is the most important part, creating the unique dynamic behavior of FPs. The chromophore is formed autocatalytically from three amino acids positioned from 65-67 (numbered Thr65-Tyr66-Gly67 in *avGFP*<sup>2</sup>) through a series of chemical modifications<sup>2,9</sup>. Due to the presence of a large polarized electron conjugation system, the chromophore can ab-

sorb a particular wavelength of light and emit fluorescent light in the visible range.

Among the many types of FPs, reversibly photoswitchable fluorescent proteins (rsFPs) have attracted much attention from scientists due to their ability to be photoswitched multiple times in a reverse manner between fluorescent and nonfluorescent states<sup>10,11</sup>. Reversible photoswitching mechanisms in such FPs are thought to be primarily related to *cis*-/*trans*-isomerization along with the protonation/deprotonation of the chromophore (Figure 1)<sup>11-13</sup>. Among GFP-like proteins, three amino acids (from 65-67) forming the chromophore can vary, but most FPs consist of Tyr66-Gly67 in this triad sequence. The hydroxyl group originating from residue Tyr66 in the chromophore structure has a notable impact on the photophysical characteristics of GFP-like proteins. Depending on various factors, such as the microenvironment of the chromophore, interactions between the chromophore and nearby residues, or the pH of the external environment,

Hanoi National University of Education

### Correspondence

Thi Yen Hang Bui, Hanoi National University of Education

Email: hangbty@hnue.edu.vn

### History

- Received: 2023-12-11
- Accepted: 2024-01-24
- Published Online: 2024-3-31

### DOI :

<https://doi.org/10.32508/stdj.v27i1.4225>



### Copyright

© VNUHCM Press. This is an open-access article distributed under the terms of the Creative Commons Attribution 4.0 International license.



**Cite this article :** Bui T Y H, Tran T N. A simple method to estimate the  $pK_a$  values of four fluorescent proteins based on measuring their pH-dependent absorbance spectra. *Sci. Tech. Dev. J.* 2024; 27(1):3286-3293.

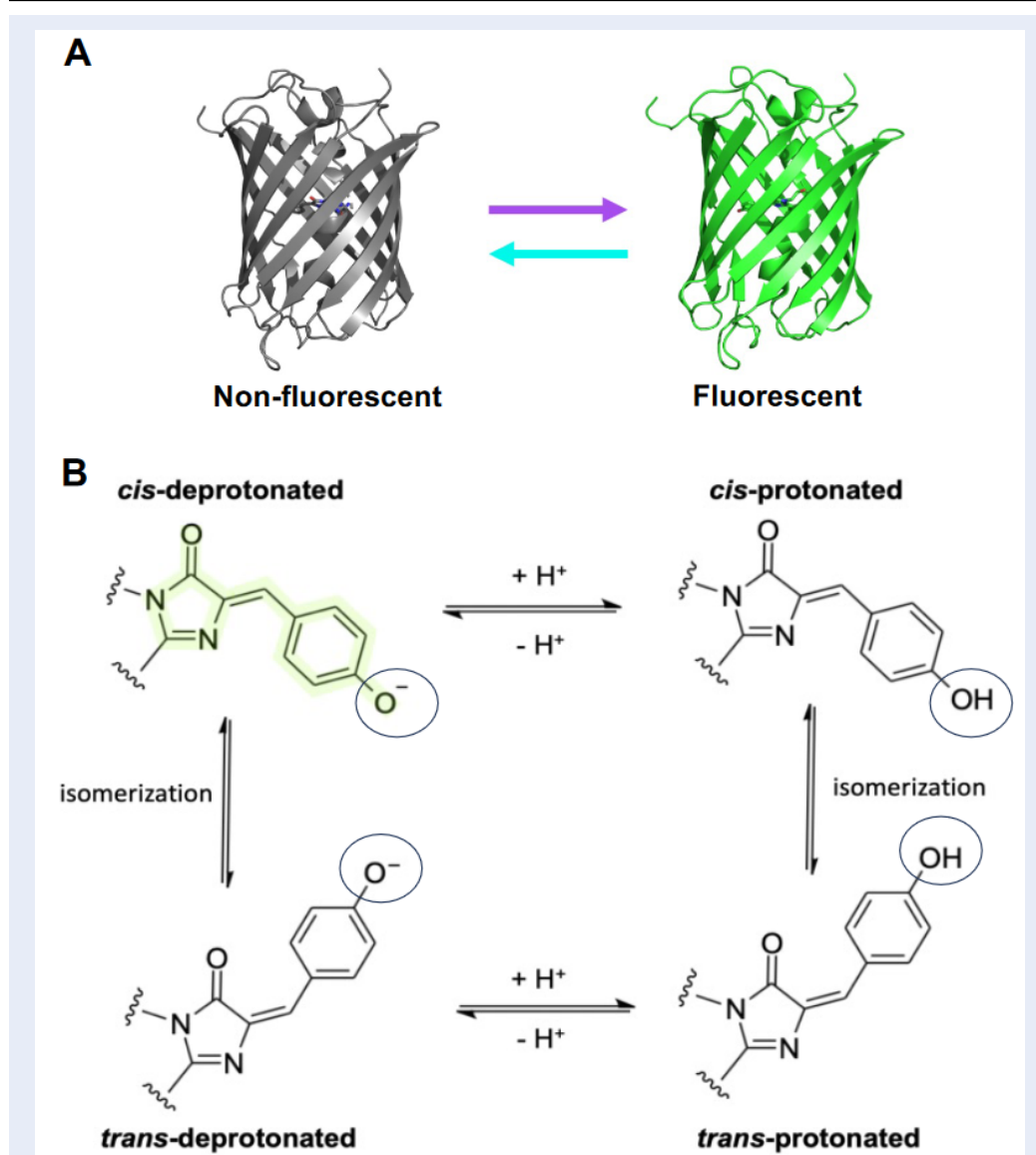


**Figure 1:** Representation of two fluorescent states in Dronpa – a green reversibly photoswitchable fluorescent protein (A) and four different forms of their chromophores with their conjugate acid–base groups circled (B). The PDB codes for fluorescent and nonfluorescent structures are 2IOV (17) and 2POX (18), respectively. The chemical structures of the chromophores were created with the ChemDraw online tool.

the hydroxyl group from Tyr66 in the chromophore-forming triad can be deprotonated or protonated, which creates an equilibrium between the neutral (protonated/acidic) and anionic (deprotonated/basic) states of the chromophore. In addition, the methylene bridge between the *p*-hydroxyphenyl and imidazolinone rings has a double bond, which allows the chromophore to occupy two distinct configurations (*cis*-/*trans*-). Therefore, the chromophore can theoretically exist in one of four states: *cis*-protonated, *cis*-deprotonated, *trans*-protonated and

*trans*-deprotonated (Figure 1B)<sup>14</sup>. The fluorescent state of rsFPs typically has a *cis*-deprotonated chromophore, whereas numerous nonfluorescent states of rsFPs primarily comprise *trans*-protonated chromophores<sup>10,11,15</sup>. The  $pK_a$  of rsFPs and the pH of the external environment strongly affect the photobehavior of such proteins by controlling the ratio between the fluorescent and nonfluorescent states<sup>16</sup>. Therefore, the  $pK_a$  is one of the crucial parameters for evaluating how effectively a rsFP can be used in specific experiments. Based on their  $pK_a$  values, scientists can

select appropriate rsFPs to study processes in acidic or alkaline environments. Determining the  $pK_a$  of the rsFP chromophore is essential for characterizing any rsFP. Most of the reported  $pK_a$  values thus far are for the *cis*-configuration of rsFPs' chromophores, and very few  $pK_a$ s of *trans*-chromophores have been published.

To date, many analytical methods, including potentiometry, conductometry, voltammetry, UV/Vis spectrometry and chromatography, have been applied to determine  $pK_a$  values<sup>17,18</sup>. However, depending on the characteristics of specific substances, some analytical methods are used more frequently than others<sup>18</sup>. For example, potentiometry can be used to determine the aqueous  $pK_a$  of a substance if the substance is sufficiently soluble in water at an appropriate pH between 2 and 12. For substances with a chromophore that is close to the acid/base group,  $pK_a$ s can be estimated in highly diluted solutions by using the spectrometry method<sup>17,18</sup>. Therefore, to determine the  $pK_a$ s of FPs, a special class of proteins with unique chromophores in the center, UV-Vis spectroscopy is one of the most commonly used methods.

In our report, the UV/Vis spectrometry method was applied to estimate the  $pK_a$  of the *cis*- and/or *trans*-chromophores of four green rsFPs, namely, GMarsQ<sup>19</sup>, Skylan-S<sup>20</sup>, Dronpa<sup>21</sup> and rsEGFP2<sup>22</sup>. We were able to obtain  $pK_a$  values for the *cis*-chromophores of GMarsQ and Skylan-S. In particular, the  $pK_a$  values for the *trans*-state of the chromophore in three rsFPs (Dronpa, GMarsQ, rsEGFP2) were also estimated, which is typically not reported in previous studies. This method is simple but efficient, which allows us to quickly obtain the  $pK_a$  values of FPs in general and rsFPs in particular.

## MATERIALS AND METHODS

### Protein expression and purification

The pRSETb plasmid containing the desired FPs was transformed into *E. coli* JM109(DE3) cells (Promega). Leak expression based on the T7 promoter controlling the inserted gene was used for this protein expression. A single colony was picked and inoculated in 1 l of LB (Lysogeny broth - Merck) medium supplemented with 100  $\mu$ g/ml ampicillin. The culture was vigorously shaken for 72 hours at a constant temperature until it was strongly colored (21°C). After being harvested, the cells were dissolved in TN 100/300 buffer (100 mM Tris-HCl pH 7.4, 300 mM NaCl) and then lysed by a French press. After that, the mixture was centrifuged for 20 min at high speed to separate the resultant cellular debris and the supernatant. The

resulting supernatant was then incubated with Ni-NTA agarose (Qiagen) for 40 min at 4°C. A Thermo Fisher Scientific Pierce polypropylene 5 ml disposable column was used for His-tag purification; the wash buffer and elution buffer used were TNi 100/300/20 (100 mM Tris-HCl pH 7.4, 300 mM NaCl, 20 mM imidazole) and TNi 100/300/250 (100 mM Tris-HCl pH 7.4, 300 mM NaCl, 250 mM imidazole), respectively. PD-10 columns (Cytiva) were used to remove high concentrations of imidazole, and the proteins were finally stored in TN 100/300 buffer for further experiments.

### Buffer preparation

To determine the dependence of the absorbance spectra of rsFP on pH, a series of universal buffers with different pH values were used. A stock of universal buffers was initially prepared using the following recipe: 50 mM citric acid, 50 mM glycine, 50 mM  $KH_2PO_4$ , 50 mM Tris-HCl and 100 mM NaCl. The buffers were then adjusted to the desired pH (from 4.0 to 12.0) using concentrated HCl and NaOH. After that, these buffers were filtered and stored at 4°C.

### $pK_a$ determination

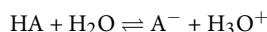
The concentrated solution of rsFPs was diluted in a series of buffers with different pH values ranging from 4.0 to 12.0, and their absorbance spectra were recorded by a miniature spectrophotometer (Ocean Optics USB-4000) in a setup described in the study of Moeyaert. B *et al.*<sup>23</sup>. The absorbance at approximately 488 nm was measured and normalized to the absorbance at 280 nm and then plotted against the pH. Each dataset was fitted to a sigmoid function (by using Igor Pro, Wavemetrics), and the apparent  $pK_a$  of the chromophore was defined as the inflection point of this curve. By titrating a solution that fully consisted of the *cis*-chromophore when unirradiated and a solution that was assumed to be entirely in the *trans*-state when irradiated with cyan light (488 nm, 60 mW, Spectra Physics), we were able to estimate the  $pK_a$  values of the *cis*- and *trans*-states, respectively. To determine the irradiation time required to convert all proteins to the dark state, aliquots of three rsFPs (Dronpa, rsEGFP2 and GMarsQ) were irradiated with cyan light for different durations. All these green rsFPs absorb strongly at approximately 480-510 nm at pH 7.4 in the initial state. When irradiated with cyan light, the proteins gradually switched from a fluorescent state with a *cis*-chromophore to a nonfluorescent state with a *trans*-chromophore, resulting in decreases in both the absorbance peak at 480-510 nm and fluorescence emission (excited at 488 nm). The proteins

were irradiated until there were no more decreases in their absorbance peaks at 480-510 nm or fluorescence emission. The green color of these rsFPs also disappeared when all proteins were photoswitched off to the dark state.

## RESULTS

### UV/Vis spectrometry method to determine $pK_a$

When an acidic HA is dissolved in water, its dissociation results in an equilibrium of acidic HA and basic  $A^-$  forms (or protonated and deprotonated forms), as follows:



This acid dissociation is characterized by an equilibrium constant called  $K_a$ , which is defined by

$$K_a = \frac{[H^+][A^-]}{[HA]} \quad (1)$$

in which  $[H^+]$ ,  $[HA]$  and  $[A^-]$  are the concentrations of the hydronium ion, acidic form and basic form at equilibrium, respectively. The total concentration  $C_T$  of acidic and basic forms (or protonated and deprotonated) in the solution is given by

$$C_T = [HA] + [A^-] \quad (2)$$

From [1] and [2], the relation between  $K_a$  and the fraction of protonated/deprotonated forms ( $f_{HA}$  and  $f_{A^-}$ ) can be represented by

$$f_{HA} = \frac{[H^+]}{[H^+] + K_a} \quad (3)$$

and

$$f_{A^-} = \frac{K_a}{[H^+] + K_a} \quad (4)$$

In addition, according to the Beer-Lambert law, UV-visible absorbance is dependent on the extinction coefficient  $\epsilon$ , concentration  $C$  and pathlength  $l$  through the following equation:

$$A = \epsilon \cdot C \cdot l \quad (5)$$

Provided that the measured absorbance of the solution is additive, it can be related to the concentration of protonated and deprotonated forms via the following equation:

$$A = \epsilon_{HA} \cdot [HA] \cdot l + \epsilon_{A^-} \cdot [A^-] \cdot l \quad (6)$$

These above equations [1-6] could be combined to give an equation representing the total absorbance of

an HA solution as a function of pH,  $pK_a$  and the extinction coefficients of its protonated and deprotonated forms as follows:

$$A = \frac{C_T l}{[H^+] + K_a} (\epsilon_{HA} \cdot [H^+] + \epsilon_{A^-} \cdot K_a) \quad (7)$$

or

$$A = \frac{C_T \cdot l}{10^{-pH} + 10^{-pH} \times (\epsilon_{HA} \cdot 10^{-pH} + \epsilon_{A^-} \cdot 10^{-pK_a})} \quad (8)$$

or

$$A = C_T l (\epsilon_{HA} \frac{1}{1 + 10^{pH-pK_a}} + \epsilon_{A^-} \frac{1}{1 + 10^{pK_a-pH}}) \quad (9)$$

As the extinction coefficient ( $\epsilon_{HA}$ ,  $\epsilon_{A^-}$ ) and path-length  $l$  are constant, it is possible to use equation [9] to estimate the  $pK_a$  by fitting a series of datasets (measured absorbance  $A$  and pH) to the sigmoid curve if the concentration  $C_T$  is unchanged. Any concentration changes in the total concentration of acidic and basic forms can be adjusted by using the ratio of the absorbances at two different wavelengths ( $\lambda_1$  and  $\lambda_2$ )<sup>18</sup>; then,  $A_{\lambda_1}/A_{\lambda_2}$  becomes concentration-independent as follows:

$$\frac{A_{\lambda_1}}{A_{\lambda_2}} = \frac{\epsilon_{HA,\lambda_1} \cdot 10^{-pH} + \epsilon_{A^-,\lambda_1} \cdot 10^{-pK_a}}{\epsilon_{HA,\lambda_2} \cdot 10^{-pH} + \epsilon_{A^-,\lambda_2} \cdot 10^{-pK_a}} \quad (10)$$

or

$$\frac{A_{\lambda_1}}{A_{\lambda_2}} = \frac{\epsilon_{HA,\lambda_1} + \epsilon_{A^-,\lambda_1} \cdot 10^{pH-pK_a}}{\epsilon_{HA,\lambda_2} + \epsilon_{A^-,\lambda_2} \cdot 10^{pH-pK_a}} \quad (11)$$

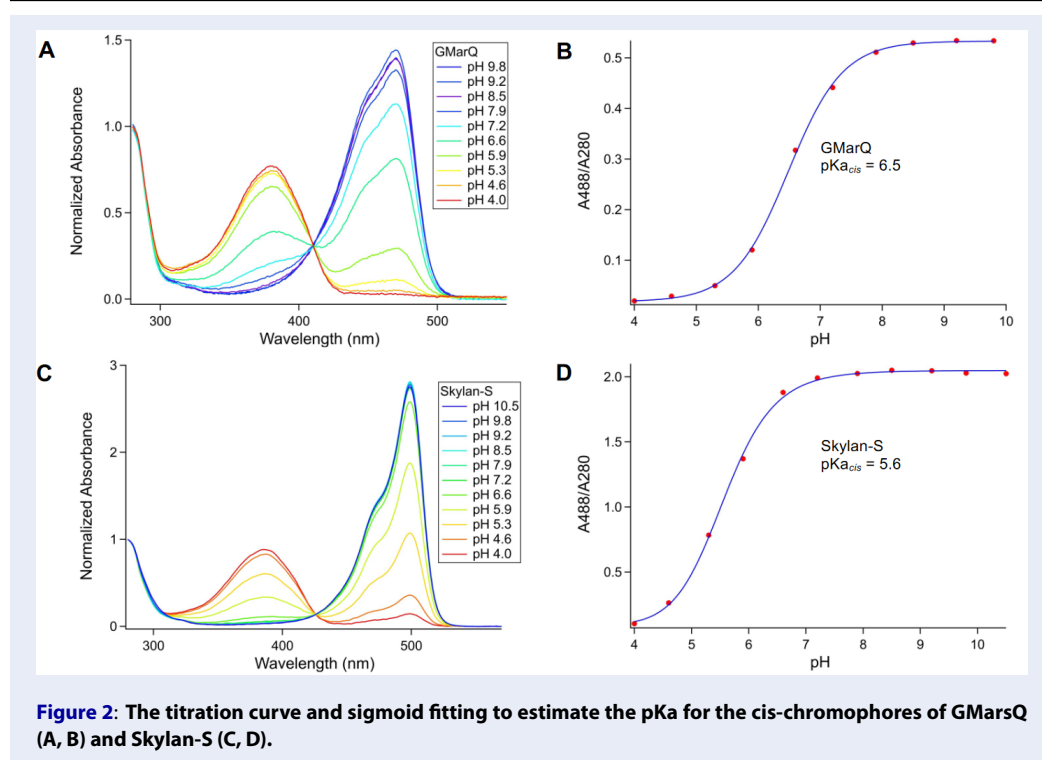
In our work, the  $pK_a$  values were estimated by measuring the absorbance spectra of rsFP in many buffers with variable pH values. The absorbance of the deprotonated chromophore (or anionic chromophore) at  $\lambda_1=488$  nm is normalized to the absorbance at  $\lambda_2=280$  nm; then, equation [11] can be written as

$$\frac{A_{488}}{A_{280}} = \frac{\epsilon_{HA,488} + \epsilon_{A^-,488} \cdot 10^{pH-pK_a}}{\epsilon_{280} + \epsilon_{280} \cdot 10^{pH-pK_a}} \quad (13)$$

According to equation [13], the relationship between  $A_{488}/A_{280}$  and pH is a sigmoid function

$$\frac{A_{488}}{A_{280}} = \frac{a + b \cdot 10^{pH-pK_a}}{1 + 10^{pH-pK_a}} \quad (14)$$

in which  $a$ ,  $b$  and  $pK_a$  are constant. The curve representing this function has an inflection point when  $pH = pK_a$ . As a result, the  $pK_a$  of a rsFP can be determined by collecting a series of absorbance spectra of this protein at different pH values and then plotting the normalized absorbance at 488 nm to 280 nm ( $A_{488}/A_{280}$ ) against the pH. Fitting this curve to a sigmoid function would result in an inflection point at the  $pK_a$  value.

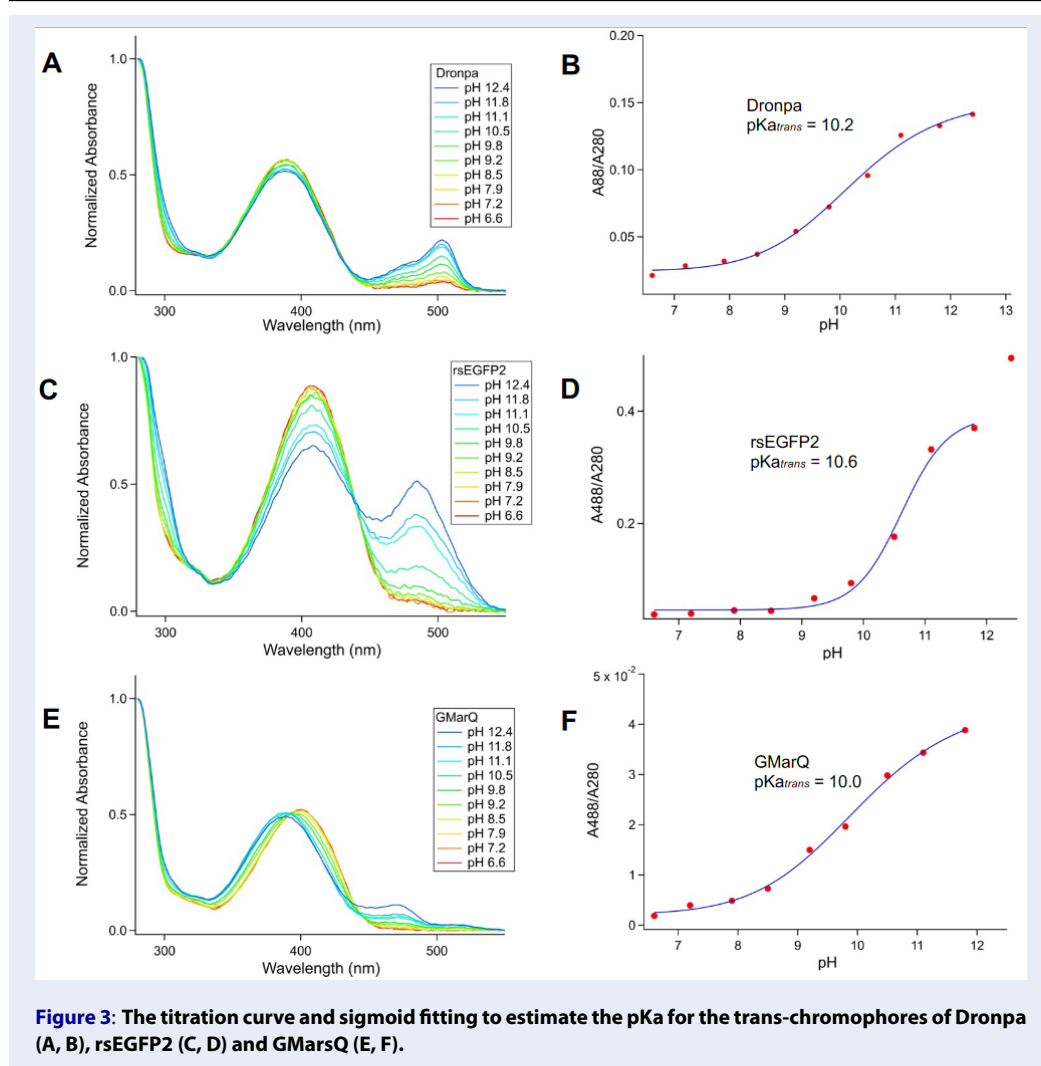


### Determination of the pK<sub>a</sub> of four rsFPs

By using this method, we were able to estimate the pK<sub>a</sub> of the *cis*-chromophore for two green rsFPs, GMarsQ (pK<sub>a</sub> = 6.5) and Skylan-S (pK<sub>a</sub> = 5.6) (Figure 2). We also tried to estimate the pK<sub>a</sub> values of the *trans*-chromophores of Dronpa, GMarsQ and rsEGFP2 (Figure 3). To obtain these *trans*-chromophore pK<sub>a</sub> values, solutions of Dronpa, rsEGFP2 and GMarsQ were irradiated with cyan light for 40 min, 5 min and 10 min, respectively, until all proteins were switched off to the dark state. The titration was quickly performed in the dark. The fitting curves of A<sub>488</sub>/A<sub>280</sub> against pH resulted in pK<sub>a</sub> values of *trans*-chromophores in these three rsFPs of approximately 10. These results demonstrate that the *trans*-chromophore is less acidic than the *cis*-chromophore and that the deprotonation of the hydroxyl group in the *trans*-chromophore is more difficult than that in the *cis*-chromophore. Among the five pK<sub>a</sub> values obtained in our work, only the pK<sub>a</sub> for the *cis*-chromophore of GMarsQ has been previously reported. In this work, the pK<sub>a</sub> for the *cis*-chromophore of GMarsQ was estimated as the pH at which the fluorescence emission reached half of the maximum, with the obtained pK<sub>a</sub> being 6.1<sup>19</sup>, which is very similar to the pK<sub>a</sub> determined by our method.

### DISCUSSION

The pK<sub>a</sub> values of the four green rsFPs in our study were estimated based on the UV/Vis spectrometry method. In this method, two requirements must be fulfilled. *First*, Beer's law needs to be satisfied for acidic and basic species so that the absorbances of these species are proportional to their concentration in solution, as mentioned in equation [5]. Hence, the dependence of the absorbance on pH is related to the dependence of the concentration on pH, which allows us to use absorbance spectra to estimate the pK<sub>a</sub>. *Second*, an unirradiated solution of a green rsFP in the thermal state is considered to be fully in the *cis*-state, and when irradiated with cyan light, this solution is switched entirely to the *trans*-state. Our work was carried out on the basis of the relationship between *cis*-/*trans*- and fluorescent/nonfluorescent states in green rsFPs, which has been confirmed in many studies<sup>10,11,14,15</sup>. The physical state of rsFPs can be examined by determining their X-ray structures. To our knowledge, the available crystal structures of green rsFPs, except Padron and Dreiklang, all demonstrate that green rsFPs in the initial state are "fluorescent" with *cis*-chromophores, and when switched to the "nonfluorescent" state, their chromophore converts to a *trans*-chromophore<sup>10,11</sup>. Currently, the crystal structures of Dronpa and rsEGFP2 (in both on-



and off-states) have been published<sup>24–27</sup>. The crystal structures of Skylan-S and GMarsQ have not yet been reported. However, Skylan-S and GMarsQ were engineered from mEos2 and mTFP1, both of which consist of *cis*-chromophores in the fluorescent state. Compared to other analytical techniques, spectrometry is the most frequently used and most effective method for estimating the  $pK_a$  values of FPs for two reasons. First, the presence of a chromophore containing an acid/base group in the structure of FPs results in significant differences in the absorbance spectra of the acidic and basic forms. Therefore, the dependence of absorbance on pH in rsFPs can be applied to estimate  $pK_a$  values in rsFPs. *Second*, as mentioned above, this method can be independent of protein concentration since the absorbance at two wavelengths is recorded to avoid the effect of concentration changes during titration. One is the absorbance

at a wavelength of 280 nm, which represents the total concentration of proteins (FPs) in a solution<sup>28</sup>, and the other is the absorbance peak at approximately 488 nm, which represents the absorbance of the deprotonated species. In principle, absorbance at any wavelength can be used in this method; however, selecting the appropriate wavelength would reduce noise from collected data and increase the accuracy of the estimation. Furthermore, similar to using the absorbance spectra, the  $pK_a$  of rsFPs can also be obtained by measuring their fluorescence intensity at different pH values and then estimating the  $pK_a$  as the pH at which the fluorescence intensity drops by one-half compared to the maximum value<sup>29,30</sup>. However, the fluorescence-based method is not suitable for determining the  $pK_a$  of *trans*-chromophores, as most rsFPs do not emit fluorescence if their chromophores adopt a *trans*-configuration.

Although this method is simple and works efficiently to estimate the  $pK_a$  of FPs, some limitations might affect the titration. As FPs can be denatured under strongly acidic or basic conditions, it is challenging to obtain accurate absorbance spectra of rsFPs at extreme pH values. A too low pH (lower than 4.0) or too high pH (higher than 12.0) can lead to incomplete titration and incorrect fitting during data processing. Moreover, issues can also occur when the unirradiated solutions of rsFPs are not fully in the *cis*-state (for example, Padron<sup>31</sup>), when the irradiated solutions are not completely in the *trans*-state due to incomplete photoswitching, or when the rsFP in the dark state returns to the bright state (by thermal recovery process) too quickly. In these cases, the titration is not reliable. In our work, the most interesting is the determination of the  $pK_a$  of the *trans*-configuration of the chromophore. To date, few  $pK_a$  values for *trans*-chromophores have been reported, and most previous publications have focused only on *cis*-chromophores<sup>32</sup>. However, these two values are critical parameters that provide further understanding of the equilibrium of the four chromophore states in the solution of a rsFP. This information would be very useful for designing FPs with desired properties that are suitable for specific experimental requirements, such as generating FPs that are highly acid resistant and base resistant in both bright and dark states. Nevertheless, some questions related to these  $pK_a$  values still exist, such as why the  $pK_a$  of *trans*-chromophores is higher than that of *cis*-chromophores, which requires further studies in the future.

## CONCLUSIONS AND PERSPECTIVES

In our report, the  $pK_a$  values for the *cis*-state and especially for the *trans*-state of some green rsFPs were estimated by applying UV/Vis spectroscopy. This approach is based on the dependence of the absorbance spectra of rsFPs on pH to estimate the  $pK_a$ . It is simple but relatively effective, which enables rapid estimation of the  $pK_a$  values of FPs generally and rsFPs specifically. However, there are still some factors affecting the estimation, and deeper studies are needed. In the future, large-scale measurements need to be performed to evaluate the accuracy and efficiency of this method in determining the  $pK_a$  values of rsFPs.

## LIST OF ABBREVIATIONS

avGFP: *Aequorea victoria* Green Fluorescent Protein  
*E. coli*: *Escherichia coli*  
 FP: Fluorescent Protein  
 GFP: Green Fluorescent Protein  
 LB: Lysogeny Broth

rsFP: Reversibly photoswitchable Fluorescent Protein  
 Tris: Tris(hydroxymethyl)aminomethane  
 UV/Vis: Ultraviolet/Visible

## COMPETING INTERESTS

The author(s) declare that they have no competing interests.

## ACKNOWLEDGEMENTS

B.T.Y.H. acknowledges support from grants from the Vietnamese government (Project 911) and the Schlumberger Foundation (Faculty for the Future Program) for her doctoral study. We thank our colleagues in the Department of Chemistry, Faculty of Science, KU Leuven, Belgium, for their support in performing the experiments and processing the data.

## REFERENCES

- Shimomura O, Johnson FH, Saiga Y. Extraction, Purification and Properties of Aequorin, a Bioluminescent Protein from the Luminous Hydromedusa, *Aequorea*. *J Cell Comp Physiol* [Internet]. 1962 Jun;59(3):223-39; PMID: 13911999. Available from: <https://doi.org/10.1002/jcp.1030590302>.
- Prasher DC, Eckenrode VK, Ward WW, Prendergast FG, Cormier MJ. Primary structure of the *Aequorea victoria* green-fluorescent protein. *Gene* [Internet]. 1992 Feb;111(2):229-33; PMID: 1347277. Available from: [https://doi.org/10.1016/0378-1119\(92\)90691-H](https://doi.org/10.1016/0378-1119(92)90691-H).
- Chudakov DM, Lukyanov S, Lukyanov KA. Fluorescent proteins as a toolkit for in vivo imaging. *Trends Biotechnol* [Internet]. 2005 Dec;23(12):605-13; PMID: 16269193. Available from: <https://doi.org/10.1016/j.tibtech.2005.10.005>.
- Chudakov DM, Matz M V., Lukyanov S, Lukyanov KA. Fluorescent proteins and their applications in imaging living cells and tissues. *Physiol Rev* [Internet]. 2010 Jul;90(3):1103-63; PMID: 20664080. Available from: <https://doi.org/10.1152/physrev.00038.2009>.
- Rodriguez EA, Campbell RE, Lin JY, Lin MZ, Miyawaki A, Palmer AE, et al. The Growing and Glowing Toolbox of Fluorescent and Photoactive Proteins. *Trends Biochem Sci* [Internet]. 2017 Feb;42(2):111-29; PMID: 27814948. Available from: <https://doi.org/10.1016/j.tibs.2016.09.010>.
- Albani JR. Principles and Applications of Fluorescence Spectroscopy [Internet]. Baldini F, Homola J, Lieberman RA, editors. Vol. 7356, Sensors (Peterborough, NH). Wiley; 2007. 735612 p; Available from: <http://proceedings.spiedigitallibrary.org/proceeding.aspx?doi=10.1117/12.822857>.
- Galbraith CG, Galbraith JA. Superresolution microscopy at a glance. *J Cell Sci* [Internet]. 2011 May 15;124(10):1607-11; PMID: 21536831. Available from: <https://doi.org/10.1242/jcs.080085>.
- Jing Y, Zhang C, Yu B, Lin D, Qu J. Super-Resolution Microscopy: Shedding New Light on In Vivo Imaging. *Front Chem* [Internet]. 2021 Sep 14;9(September):1-18; PMID: 34595156. Available from: <https://doi.org/10.3389/fchem.2021.746900>.
- Ormö M, Cubitt AB, Kallio K, Gross LA, Tsien RY, Remington SJ. Crystal Structure of the *Aequorea victoria* Green Fluorescent Protein. *Science* (80) [Internet]. 1996 Sep 6;273(5280):1392-5; PMID: 8703075. Available from: <https://doi.org/10.1126/science.273.5280.1392>.
- Bourgeois D, Adam V. Reversible photoswitching in fluorescent proteins: A mechanistic view. *IUBMB Life* [Internet]. 2012 Jun;64(6):482-91; PMID: 22535712. Available from: <https://doi.org/10.1002/iub.1023>.

11. Nienhaus K, Nienhaus GU. Photoswitchable Fluorescent Proteins: Do Not Always Look on the Bright Side. *ACS Nano* [Internet]. 2016 Oct 25;10(10):9104-8;PMID: 27723301. Available from: <https://doi.org/10.1021/acsnano.6b06298>.
12. Adam V, Berardozi R, Byrdin M, Bourgeois D. Phototransformable fluorescent proteins: Future challenges. *Curr Opin Chem Biol* [Internet]. 2014 Jun;20(1):92-102;PMID: 24971562. Available from: <https://doi.org/10.1016/j.cbpa.2014.05.016>.
13. Tang L, Fang C. Photoswitchable Fluorescent Proteins: Mechanisms on Ultrafast Timescales. *Int J Mol Sci* [Internet]. 2022 Jun 9;23(12):6459;PMID: 35742900. Available from: <https://doi.org/10.3390/ijms23126459>.
14. Nienhaus K, Nienhaus GU. Genetically encodable fluorescent protein markers in advanced optical imaging. *Methods Appl Fluoresc* [Internet]. 2022 Oct 1;10(4):042002;PMID: 35767981. Available from: <https://doi.org/10.1088/2050-6120/ac7d3f>.
15. Rodrigues EC, Stiel AC. It's a two-way street: Photoswitching and reversible changes of the protein matrix in photoswitchable fluorescent proteins and bacteriophytochromes. *FEBS Lett* [Internet]. 2023 May 10;597(10):1319-44;PMID: 36915180. Available from: <https://doi.org/10.1002/1873-3468.14609>.
16. Campbell TN, Choy FYM. The effect of pH on green fluorescent protein: A brief review. *Mol Biol Today*. 2001;2(1):1-4; Available from: <https://www.caister.com/backlist/mbt/v/v2/01.pdf>.
17. Reijenga J, van Hoof A, van Loon A, Teunissen B. Development of methods for the determination of pKa values. *Anal Chem Insights*. 2013;8(1):53-71;PMID: 23997574. Available from: <https://doi.org/10.4137/ACLS12304>.
18. Subirats X, Fuguet E, Rosés M, Bosch E, Rafols C. Methods for pKa Determination (I): Potentiometry, Spectrophotometry, and Capillary Electrophoresis. *Ref Modul Chem Mol Sci Chem Eng*. 2015;(October 2017); Available from: <https://doi.org/10.1016/B978-0-12-409547-2.11559-8>.
19. Wang S, Chen X, Chang L, Xue R, Duan H, Sun Y. GMars-Q Enables Long-Term Live-Cell Parallelized Reversible Saturable Optical Fluorescence Transitions Nanoscopy. *ACS Nano* [Internet]. 2016 Oct 25;10(10):9136-44;PMID: 27541837. Available from: <https://doi.org/10.1021/acsnano.6b04254>.
20. Zhang X, Chen X, Zeng Z, Zhang M, Sun Y, Xi P, et al. Development of a Reversibly Switchable Fluorescent Protein for Super-Resolution Optical Fluctuation Imaging (SOFI). *ACS Nano* [Internet]. 2015 Mar 24;9(3):2659-67;PMID: 25695314. Available from: <https://doi.org/10.1021/nn5064387>.
21. Ando R, Mizuno H, Miyawaki A. Regulated Fast Nucleocytoplasmic Shuttling Observed by Reversible Protein High-lighting. *Science* (80) [Internet]. 2004 Nov 19;306(5700):1370-3;PMID: 15550670. Available from: <https://doi.org/10.1126/science.1102506>.
22. Grotjohann T, Testa I, Reuss M, Brakemann T, Eggeling C, Hell SW, et al. rsEGFP2 enables fast RESOLFT nanoscopy of living cells. *Elife* [Internet]. 2012 Dec 31;1(1):1-14;PMID: 23330067. Available from: <https://doi.org/10.7554/eLife.00248>.
23. Moeyaert B, Nguyen Bich N, De Zitter E, Rocha S, Clays K, Mizuno H, et al. Green-to-Red Photoconvertible Dronpa Mutant for Multimodal Superresolution Fluorescence Microscopy. *ACS Nano* [Internet]. 2014 Feb 25;8(2):1664-73;PMID: 24410188. Available from: <https://doi.org/10.1021/nn4060144>.
24. Stiel AC, Trowitzsch S, Weber G, Andresen M, Eggeling C, Hell SW, et al. 1.8 Å bright-state structure of the reversibly switchable fluorescent protein Dronpa guides the generation of fast switching variants. *Biochem J* [Internet]. 2007 Feb 15;402(1):35-42;PMID: 17117927. Available from: <https://doi.org/10.1042/BJ20061401>.
25. Andresen M, Stiel AC, Trowitzsch S, Weber G, Eggeling C, Wahl MC, et al. Structural basis for reversible photoswitching in Dronpa. *Proc Natl Acad Sci* [Internet]. 2007 Aug 7;104(32):13005-9;PMID: 17646653. Available from: <https://doi.org/10.1073/pnas.0700629104>.
26. Wilmann PG, Turcic K, Battad JM, Wilce MCJ, Devenish RJ, Prescott M, et al. The 1.7 Å Crystal Structure of Dronpa: A Photoswitchable Green Fluorescent Protein. *J Mol Biol* [Internet]. 2006 Nov;364(2):213-24;PMID: 17010376. Available from: <https://doi.org/10.1016/j.jmb.2006.08.089>.
27. Mantovanelli AMR, Glushonkov O, Adam V, Wulffélé J, Thédié D, Byrdin M, et al. Photophysical Studies at Cryogenic Temperature Reveal a Novel Photoswitching Mechanism of rsEGFP2. *J Am Chem Soc*. 2023;145(27):14636-46;PMID: 37389576. Available from: <https://doi.org/10.1021/jacs.3c01500>.
28. Layne E. [73] Spectrophotometric and turbidimetric methods for measuring proteins. *Methods Enzymol*. 1957;3(C):447-54;PMID: 13437204. Available from: [https://doi.org/10.1016/S0076-6879\(57\)03413-8](https://doi.org/10.1016/S0076-6879(57)03413-8).
29. Costantini LM, Baloban M, Markwardt ML, Rizzo MA, Guo F, Verkhusha V V, et al. A palette of fluorescent proteins optimized for diverse cellular environments. *Nat Commun* [Internet]. 2015 Jul 9;6(1):7670;PMID: 26158227. Available from: <https://doi.org/10.1038/ncomms8670>.
30. Zhang M, Chang H, Zhang Y, Yu J, Wu L, Ji W, et al. Rational design of true monomeric and bright photoactivatable fluorescent proteins. *Nat Methods*. 2012;9(7):727-9;PMID: 22581370. Available from: <https://doi.org/10.1038/nmeth.2021>.
31. Andresen M, Stiel AC, Fölling J, Wenzel D, Schönle A, Egnér A, et al. Photoswitchable fluorescent proteins enable monochromatic multilabel imaging and dual color fluorescence nanoscopy. *Nat Biotechnol* [Internet]. 2008 Sep 24;26(9):1035-40;PMID: 18724362. Available from: <https://doi.org/10.1038/nbt.1493>.
32. Cranfill PJ, Sell BR, Baird MA, Allen JR, Lavagnino Z, De Gruiter HM, et al. Quantitative assessment of fluorescent proteins. *Nat Methods*. 2016;13(7):557-62;PMID: 27240257. Available from: <https://doi.org/10.1038/nmeth.3891>.